CPSO based LFC for a Two-area Power System with GDB and GRC Nonlinearities Interconnected through TCPS in Series with the Tie-Line

R. Arivoli
Associate Professor
Department of Electrical Engineering,
Annamalai University
Annamalainagar – 608002.
Tamilnadu, India

Dr. I. A. Chidambaram
Professor
Department of Electrical Engineering,
Annamalai University,
Annamalainagar – 608002.
Tamilnadu, India

ABSTRACT

In this paper the design of Proportional Integral (PI) controller is proposed using Craziness Particle Swarm Optimization (CPSO) based Integral Square Error (CPSOISE), CPSO based Apex Stability Verge (CPSOASV) and Multi-Objective based CPSO (MOCPSO) are used to design the controller for a two-area power system considering Governor Dead Band (GDB) and Generation Rate Constraint (GRC) nonlinearities coordinate with Super Conducting Magnetic Energy Storage (SMES) units and interconnected through Thyristor Controlled Phase Shifter (TCPS). CPSO algorithm is a powerful optimum search technique, the salient advantage is that it is highly insensitivity to large load changes and disturbances in the presence of plant parameter variations and system nonlinearities under load following variations. For the proposed method, two types of controllers namely, Mutual Aid Criterion (MAC) based Integral Square Error (ISE) and Apex Stability Verge (ASV) controllers are designed first and then the proposed MOCPSO controller is designed. Simulation results of the proposed MOCPSO controller is not only effective in damping out frequency oscillations, but also capable of alleviating the transient frequency swing caused by the disturbances. From the dynamic responses it reveals that the MOCPSO based controller for the two area reheat power system with SMES, interconnected with TCPS ensures better transient performance and faster settling time than that of the CPSOISE based controller.

General Terms

Load-Frequency Control (LFC), PI controller, Mutual Aid Criterion (MAC), Craziness Particle Swarm Optimization (CPSO), Integral Square Error (ISE), Super Conducting Magnetic Energy Storage (SMES), Thyristor Controlled Phase Shifter (TCPS), Governor Dead Band (GDB), Generation Rate Constraint (GRC).

Keywords

Apex Stability Verge (ASV), Craziness Particle Swarm Optimization based Apex Stability Verge (CPSOASV), CPSO based Integral Square Error (CPSOISE), Multi-Objective CPSO (MOCPSO).

1. INTRODUCTION

Increase in Generation, Transmission and Utilization of modern power system has led the system to more complex. Hence the power supply with stability and high reliability is essential. Load-Frequency Control (LFC) is a very important problem in power system operation and control by which a balance between electric power generation and power consumption is maintained. Existing power system consists of many control areas interconnected together and power is exchanged between control areas through tie-lines by which they are connected. LFC plays a significant role in the power system by maintaining scheduled system frequency and tie-line flow during normal operating condition and also during small load perturbations. The stability of the inter-area oscillation mode is deteriorated by the heavy load condition in tie-lines especially due to the electric power exchange. The Load Frequency Control (LFC) problem is of vital importance in electrical power system design/operation and attention has been directed towards designing efficient controllers to ensure reliable and quality power supply. There has been considerable effort devote to LFC of interconnected power systems in the literature [1, 2]. To ensure dynamic performance of the power system, a number of control strategies have been employed in the design of load frequency controllers. The application of decentralized control strategy to the LFC problem has found wide acceptance because of its role in eliminating most of the problems associated with other centralized or multilevel control strategies [3-9].

This paper focuses on the analysis carried out for the AGC of a two-area interconnected thermal power system considering TCPS in series with the tie-line. Investigations are also carried out to examine the capability of the TCPS damping controller in two-area interconnected power system. An interconnected thermal system involves widely different characteristics for the thermal systems. The characteristics of steam turbines is that the relatively large inertia used as a source of energy causes a considerable greater time lag in the response of the change in the prime mover torque to a change in gate position, and also a non-minimum phase behaviour, that is, an initial tendency for the torque to change in a direction opposite to that finally produced. Moreover, the maximum permissible generation rate constraint for the thermal units. Further, the effects of different generation rate constraints on the selection of optimum controller settings for the thermal two areas and on the system dynamic performance considering a TCPS in series with the tie-line can be established efficiently.

In view of the above, the main objectives of the present work are:

1. To design the controller for a two-area power system considering Governor Dead Band (GDB) and Generation Rate Constraint (GRC) nonlinearities coordinate with Super

Conducting Magnetic Energy Storage (SMES) units and interconnected through Thyristor Controlled Phase Shifter (TCPS).

2. To minimise the oscillations in the system frequency and tie-line power considering a TCPS in series with the tie-line of a two-area interconnected thermal power system.

3. To optimise the gain settings of the Proportional-Integral controllers using CPSOISE, CPSOASV and MOCPSO.

4. To compare the dynamic responses.

For the past several decades, lot of work pertaining to the design of classical controllers for interconnected power systems [3-7] has been carried-out and in most of the cases, the mathematical model has been over simplified by ignoring the simultaneous presence of important system nonlinearities such as Governor Dead Band (GDB) and Generation Rate Constraints (GRC). All governors in the thermal reheat power system have deadbands like mechanical friction, backlash, valve overlaps in hydraulic relays, which are important for speed control even under small disturbances. So, the speed governor deadband has significant effect on the dynamic performance of load-frequency control system. Moreover, the GDB has a destabilizing effect on the transient response of the system [6, 8].
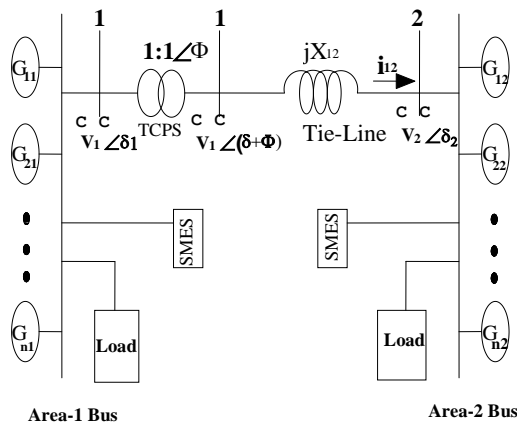

Figure 1.Two - area thermal power system with TCPS

In a power system, another most important constraint on modern large size thermal units is the stringent generation rate constraint *i.e.* the power generation can change only at a specified maximum rate. The GRC of the system is considered by adding a limiter to the control system. In this condition, the response will be with larger overshoots and longer settling times when compared with the system where GRC is not considered. So, if the parameters of the controller are not chosen properly, the system may become unstable. In the simultaneous presence of GDB and GRC, even with small load perturbation, the system becomes highly nonlinear and hence the optimization problem becomes rather complex. Many control strategies have been employed in the design of load-frequency controller for interconnected power systems considering GDB and GRC nonlinearities.

First Craziness Particle Swarm Optimization based PI controller on the basis of the cost functions using MAC is designed. Secondly MAC based PI controller on the basis of the settling time of the output frequency deviation response

for 1% step load disturbance in area 1 is designed. The first controller is referred as CPSOISE controller and the second is referred as CPSOASV controller.

The gains K_P, K_I of CPSOISE and CPSOASV controllers will be the lower and upper or upper and lower limits of the proposed MOCPSO controller. This paper investigates the performance of the MOCPSO controller in a two-area power system interconnected with TCPS. From the simulated results the controller designed based on MOCPSO ensures better transient performance and faster settling time than that of the controller designed with CPSOISE.

2. STATEMENT OF THE PROBLEM

The state variable equation of the minimum realization model of the two-area inter connected power system is expressed as

$$\dot{X}=Ax+Bu+\Gamma d \qquad (1)$$

$$\overline{X} = \{ \begin{array}{c} \int ACE_1, \ \int ACE_2, \Delta f_1, \Delta P_{G1}, \Delta P'_{G1}, \Delta X_{E1}, \\ \Delta \varphi, \Delta P_{tie}, \Delta f_2, \Delta P_{G2}, \Delta P'_{G2}, \Delta X_{E2} \} \end{array}$$

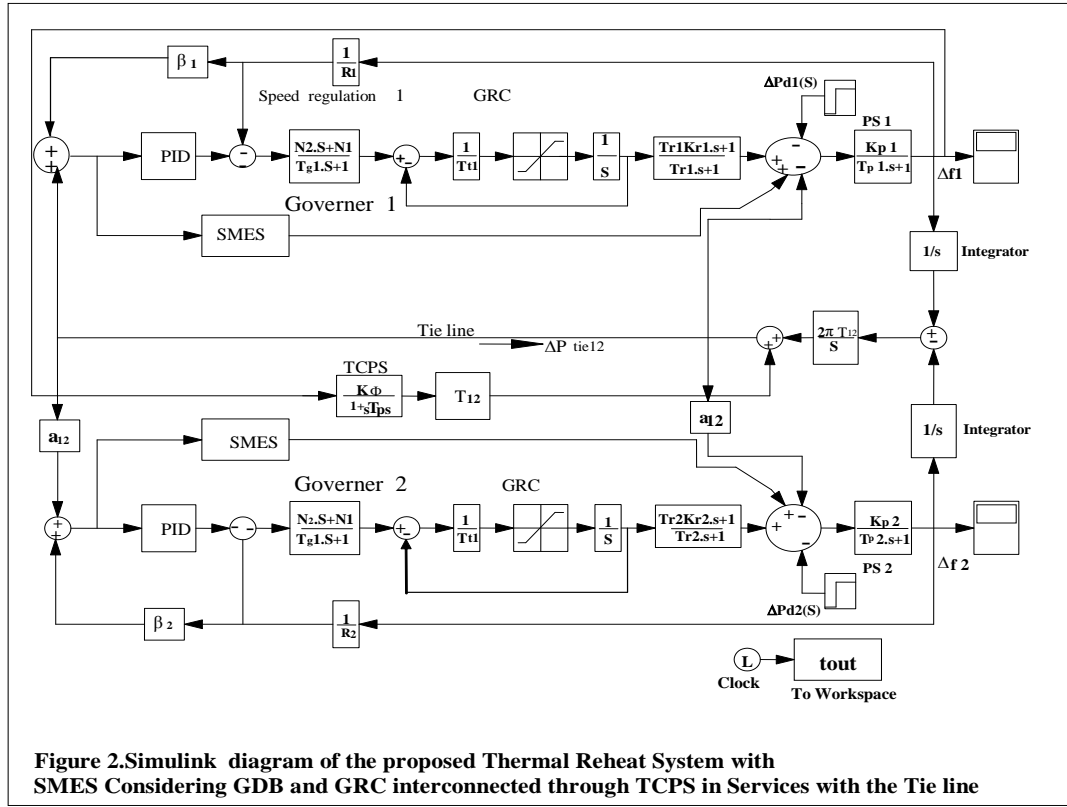$$U = [U_1, U_2]^T = [\Delta P_{C1}, \Delta P_{C2}]^T$$

$$d = [d_1, d_2]^T = [\Delta P_{D1}, \Delta P_{D2}]^T$$

Where A is the system matrix, B is the input distribution matrix, Γ is the distribution disturbance matrix, x is the state vector, u is the control vector and d is the disturbance vector due to change in load.

3. POWER SYSTEM MODEL FOR SIMULATION ANALYSIS

The AGC system investigated comprises of an interconnection of two areas, both areas comprising of a nonreheat thermal units. Fig. 1 shows the schematic of two-area interconnected thermal power system with TCPS. Two areas are connected by a weak tie-line. TCPS is placed in series with the tie-line near area-1. A TCPS is a device that changes the relative phase angle between the system voltages [14]. Therefore, the real power flow can be regulated to mitigate the frequency oscillations and enhance power system stability. The small perturbation transfer function block diagram of Fig. 1 is shown in Fig. 2. When there is sudden rise in power demand in a control area, the governor control mechanism starts working to set the power system to the new equilibrium condition. Similar action happens when there is a sudden decrease in load demand. Basically, the operation speed of governor-turbine system is slow compared with that of the excitation system. As a result, fluctuations in terminal voltage can be corrected by the excitation system very quickly, but fluctuations in generated power or frequency are corrected slowly. Since load frequency control is primarily concerned with the real power/frequency behaviour, the excitation system model will not be required in the approximated analysis [15]. This important simplification paves the way for constructing the simulation model shown in Fig. 2. The basic objective of the supplementary control in Fig. 2 is to restore balance between each area load and generation for a load disturbance. This is met when the control action maintains the frequency and the tie-line power interchange at the scheduled values.

Figure 2.Simulink diagram of the proposed Thermal Reheat System with SMES Considering GDB and GRC interconnected through TCPS in Services with the Tie line

4. STATE SPACE MODEL

For a two-area thermal reheat interconnected power system
The following equation can be written

$$\Delta \dot{F}_1 = \frac{k_{p1}}{T_{p1}}\left(\Delta P_{G1} - \Delta P_{D1} - \Delta P_{tie,1}\right) - \frac{\Delta F_1}{T_{p1}} \quad (2)$$

$$\Delta \dot{P}'_{G1} = -\frac{1}{T_{t1}}\Delta X_{E1} - \frac{1}{T_{t1}}\Delta P'_{G1} \quad (3)$$

$$\Delta \dot{P}_{G1} =$$
$$-\frac{1}{T_{r1}}\Delta P_{G1} + \frac{1}{T_{r1}} - \frac{k_{r1}}{T_{t1}} \quad \Delta P'_{G1} + \frac{K_{r1}}{T_{t1}}\Delta X_{E1} \quad (4)$$

$$\Delta \dot{X}_{E1} = -\frac{1}{T_{g1}}\Delta X_{E1} +$$
$$\frac{1}{T_{g1}}\Delta P_{c1} - \frac{1}{T_{g1}R_1}\Delta F_1 \quad (5)$$

$$\Delta \dot{P}_{tie,1} = T_{12}\left(\Delta F_1 - \Delta F_2\right) \quad (6)$$

$$\Delta \dot{F}_2 = \frac{k_{p2}}{T_{p2}}$$
$$\left(\Delta P_{G2} - \Delta P_{D2} - a_{12}\Delta P_{tie,1}\right) - \frac{\Delta F_2}{T_{p2}} \quad (7)$$

$$\Delta \dot{P}_{G2} =$$
$$-\frac{1}{T_{r2}}\Delta P_{G2} + \frac{1}{T_{r2}} - \frac{k_{r2}}{T_{t2}} \quad \Delta P'_{G2} + \frac{k_{r2}}{T_{t2}}\Delta X_{E2} \quad (8)$$

$$\Delta \dot{P}'_{G2} = -\frac{1}{T_{t2}}\Delta X_{E2} - \frac{1}{T_{t2}}\Delta P'_{G2} \quad (9)$$

$$\Delta \dot{X}_{E2} =$$
$$-\frac{1}{T_{g2}}\Delta X_{E2} + \frac{1}{T_{g2}}\Delta P_{c2} - \frac{1}{T_{g2}R_2}\Delta F_2 \quad (10)$$

$$\Delta \dot{F}_1 =$$
$$\frac{K_{p1}}{T_{p1}}\left(\Delta P_{G1} - \Delta P_{D1} - \Delta p_{ac1} - \Delta p_{dc1}\right) - \frac{\Delta F_1}{T_{p1}} \quad (11)$$

$$\Delta \dot{P}_{G1} = \frac{1}{T_{r1}}\Delta P_{G1} +$$
$$\frac{1}{T_{r1}} \quad \frac{k_{r1}}{T_{t1}} \quad \Delta P'_{G1} + \frac{K_{r1}}{T_{t1}}\Delta X_{E1} \quad (12)$$

$$\Delta \dot{P}'_{G1} = -\frac{1}{T_{t1}}\Delta X_{E1} - \frac{1}{T_{t1}}\Delta P'_{G1} \quad (13)$$

$$\Delta \dot{X}_{E1} =$$
$$- \frac{1}{T_{g1}} \Delta X_{E1} + \frac{1}{T_{g1}} \Delta P_{c1} - \frac{1}{T_{g1} R_1} \Delta F_1 \qquad (14)$$

$$ACE_1 = \beta_1 \Delta F_1 + \Delta P_{ac1} + \Delta P_{dc1} \qquad (15)$$

$$\Delta \dot{P}_{tie1,2} = 2\pi T_{12} (\Delta F_1 - \Delta F_2) \qquad (16)$$

$$\Delta \dot{F}_2 =$$
$$\frac{K_{p2}}{T_{p2}} (\Delta P_{G2} - \Delta P_{D2} - \Delta P_{ac2} - \Delta P_{dc2}) - \frac{\Delta F_2}{T_{p2}} \qquad (17)$$

$$= \frac{k_{p2}}{T_{p2}} (\Delta P_{G2} - \Delta P_{D2} - a_{12}\Delta P_{ac1} - a_{12}\Delta P_{dc1}) - \frac{\Delta F_2}{T_{p2}} \qquad (18)$$

$$\Delta \dot{P}_{G2} = -\frac{1}{T_{r2}} \Delta P_{G2} + \frac{1}{T_{r2}} \frac{k_{r2}}{T_{t2}} \Delta P'_{G2} + \frac{K_{r2}}{T_{t2}} \Delta X_{E2} \qquad (19)$$

$$\Delta \dot{P}'_{G2} = -\frac{1}{T_{t2}} \Delta X_{E2} - \frac{1}{T_{t2}} \Delta P'_{G2} \qquad (20)$$

$$\Delta \dot{X}_{E2} = -\frac{1}{T_{g2}} \Delta X_{E2} +$$
$$\frac{1}{T_{g2}} \Delta P_{c2} - \frac{1}{T_{g2} R_2} \Delta F_2 \qquad (21)$$

5. INCREMENTAL TIE-LINE POWER FLOW MODEL CONSIDERING TCPS

As the recent advances in power electronics have led to the development of the FACTS devices. Which are designed to overcome the limitations of the mechanically controlled devices used in the power systems and enhance power system stability using reliable and high-speed electronic components. One of the promising FACTS devices is the TCPS. TCPS is a device that changes the relative phase angle between the system voltages. Therefore the real power flow can be regulated to mitigate the frequency oscillations and enhance power system stability.

In this study, a two-area thermal power system interconnected by a tie-line is considered. Fig. 1 shows the schematic representation of the two-area interconnected thermal system considering a TCPS in series with the tie-line. TCPS is placed near Area 1. Practically, in an interconnected power system, the reactance-to-resistance ratio of a tie-line is quite high (X/R≥10) and the effect of resistance on the dynamic performance is not that significant. Because of this, the resistance of the tie-line is neglected. Two Area interconnected thermal power system comprising . Without TCPS, the incremental tie-line power flow from Area 1 to Area 2 can be expressed as [25]

$$\Delta P^0_{tie12} = \frac{2\pi T^0_{12}}{s} (\Delta f_1 - \Delta f_2) \qquad (22)$$

Where $T°12$ is the synchronising power coefficient without TCPS and $\Delta f1$ and $\Delta f2$ are the frequency deviations of Areas 1 and 2, respectively. When a TCPS is placed in series with the tie-line, as in Fig. 1, the current flowing from Area 1 to Area 2 can be written as

$$i_{12} = \frac{|V_1| \angle(\delta_1 + \varphi) - |V_2| \angle \delta_2}{jX_{12}} \qquad (23)$$

From Fig. 1, it can be written as

$$P_{tie12} - jQ_{tie12} = V_1^* i_{12} =$$
$$|V_1| \angle -(\delta_1 + \varphi) \left[\frac{|V_1| \angle(\delta_1 + \varphi) |V_2| \angle \delta_2}{jx_{12}} \right] \qquad (24)$$

$$P_{tie12} - jQ_{tie12} =$$
$$\frac{|V_1||V_2|}{X_{12}} \sin(\delta_1 - \delta_2 + \varphi) -$$
$$j \frac{|V_1|^2 - |V_1||V_2| \cos(\delta_1 - \delta_2 + \varphi)}{X_{12}} \qquad (25)$$

Separating the real part of (25), we get

$$P_{tie12} = \frac{|V_1||V_2|}{x_{12}} \sin(\delta_1 - \delta_2 + \varphi) \qquad (26)$$

In (26), perturbing and w from their nominal values δ_1, δ_2 and φ from their nominal values δ_1°, δ_2° and φ°, respectively, eqn. (22) now becomes

$$\Delta P_{tie12} = \frac{|V_1||V_2|}{x_{12}} \cos(\delta_1^0 - \delta_2^0 +$$
$$\phi^0 \sin(\Delta\delta_1 - \Delta\delta_2 + \Delta\phi) \qquad (27)$$

However, for a small change in real power load, the variation of bus voltage angles and also the variation of TCPS phase

angle are very small. Thus, in effect, ($\Delta\delta_1 - \Delta\delta_2 + \Delta\varphi$)

is very small and hence

$$\sin(\Delta\delta_1 - \Delta\delta_2 + \Delta\varphi) = (\Delta\delta_1 - \Delta\delta_2 + \Delta\varphi)$$

(28)

Therefore
$$\Delta P_{tie12} =$$
$$\frac{|V_1||V_2|}{x_{12}} \cos(\delta_1^0 - \delta_2^0 + \varphi^0)(\Delta\delta_1 - \Delta\delta_2 + \Delta\varphi) \qquad (29)$$

Let

$$T_{12} = \frac{|V_1||V_2|}{x_{12}} \cos(\delta_1^0 - \delta_2^0 + \varphi^0) \qquad (30)$$

Thus (29) reduces to

$$\Delta P_{tie12} = T_{12}(\Delta\delta_1 - \Delta\delta_2 + \Delta\varphi)$$

(31)

$$\Delta P_{tie12} = T_{12}(\Delta\delta_1 - \Delta\delta_2 + T_{12}\Delta\varphi) \quad (32)$$

It is Known

$$\Delta\delta_1 = 2\pi \int \Delta f_1 dt$$

and

$$\Delta\delta_2 = 2\pi \int \Delta f_2 dt \quad (33)$$

From (32) and (33)

$$\Delta P_{tie12} =$$

$$2\pi T_{12}\left(\left(\int\Delta f_1 dt - \int\Delta f_2 dt \right)\right) + T_{12}\Delta \phi \quad (34)$$

Laplace transformation of (34) yields

$$\Delta P_{tie12}(s) = \frac{2\pi T_{12}}{s}\left([\Delta F_1(s) - \Delta F_2(s)] \right) + T_{12}\Delta\phi(s) \quad (35)$$

As per (35), tie-line power flow can be controlled by controlling the phase shifter angle $\Delta\varphi$. Assuming that the control input signal to the TCPS damping controller is $\Delta Error1(s)$ and that the transfer function of the signalling conditioning circuit is $k_\varphi c(s)$, where k_φ is the gain of the TCPS controller

$$\Delta\varphi(s) = K_\varphi\, C(s)\Delta(s)\Delta Error_1(s) \quad (36)$$

And

$$C(s) = \frac{1}{1 + sT_{ps}} \quad (37)$$

Hence, the phase shifter angle $\Delta\varphi(s)$ can be represented as [13, 16]

$$\Delta\varphi(s) = \frac{K_\varphi}{1 + sT_{ps}}\Delta Error_1(s) \quad (38)$$

where T_{ps} is the time constant of the TCPS and $\Delta Error1(s)$ the control signal which controls the phase angle of the phase shifter. Thus (35) can be rewritten as

$$\Delta P_{tie12}(s) = \frac{2\pi T_{12}}{s}[\Delta F_1(s) - \Delta F_2(s)] +$$

$$T_{12}\frac{K_\phi}{1 + sT_{ps}}\Delta Error_1(s) \quad (39)$$

5.1 TCPS control strategy

$\Delta Error1$ can be any signal such as the thermal area frequency deviation $\Delta f1$ or the area control error of the thermal area ACE1 (i.e. $\Delta Error1 = \Delta f1$ or ACE1) to the TCPS unit to control the TCPS phase shifter angle which in turn controls the tie-line power flow. Thus, with $\Delta Error1 = \Delta f1$

$$\Delta\varphi(s) = \frac{K_\varphi}{1 + sT_{ps}}\Delta f_1(s)$$

(40)

and the tie-line power flow perturbation as given by (39) becomes

$$\Delta P_{tie12}(s) = \frac{2\pi T_{12}}{s}[\Delta F_1(s) - \Delta F_2(s)] +$$

$$T_{12}\frac{K_\phi}{1 + sT_{ps}}\Delta F_1(s) \quad (41)$$

When the area control error of area 1, $ACE_1 = B_1\Delta f_1 + \Delta p_{tie12}$ is chosen as the control signal (i.e. Error1 = ACE1), to the TCPS unit, the tie-line power flow perturbation becomes

$$\Delta P_{tie12}(s) = \frac{2\pi T_{12}}{s}[\Delta F_1(s) - \Delta F_2(s)] +$$

$$T_{12}\frac{K_\varphi}{1 + T_{ps}}\Delta ACE_1(s) \quad (42)$$

However, from the practical point of view, as TCPS is placed near Area 1, measurement of $\Delta f1$ will be easier rather than ACE1, which requires measurement of tie-power also. Hence, in the present work, the frequency deviation of the thermal area $\Delta f1$ is chosen as the control signal. The parameter T_{PS} and k_φ of the TCPS are given in Appendix 1.

However, from the practical point of view, as TCPS is placed near Area 1, measurement of $\Delta f1$ will be easier rather than ACE1, which requires measurement of tie-power also. Hence, in the present work, the frequency deviation of the thermal area $\Delta f1$ is chosen as the control signal. The parameter T_{PS} and k_φ of the TCPS are given in Appendix 1.

6. SUPER CONDUCTING MAGNETIC ENERGY STORAGE (SMES) DEVICE

Superconducting Magnetic Energy Storage (SMES) unit with a self-commutated converter is capable of controlling both the active and reactive power simultaneously and quickly, increasing attention has been focused recently on power system stabilization by SMES control [11].
The schematic diagram in Figure 3 shows the configuration of a thyristor controlled SMES unit. The SMES unit contains DC superconducting Coil and converter which is connected by Y–D/Y–Y transformer. The inductor is initially charged to its rated current Id0 by applying a small positive voltage. Once the current reaches the rated value, it is maintained constant by reducing the voltage across the inductor to zero since the coil is superconducting. Neglecting the transformer and the converter losses, the DC voltage is given by
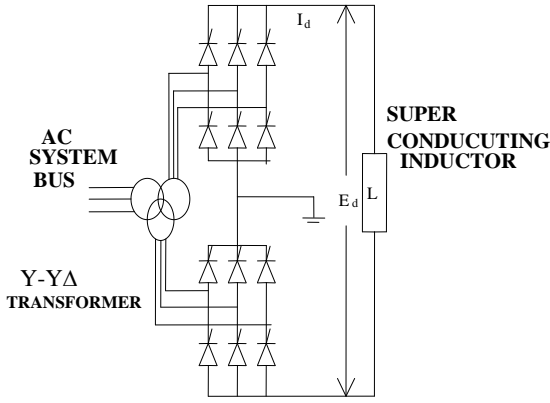
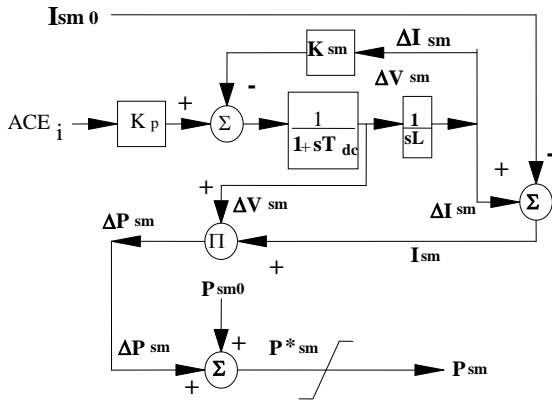Ed= 2Vd0 cos α- 2IdRc (43)

Figure 3.The Schematic diagram of SMES unit.

Figure 4. SMES control system in each area.

Where Ed is DC voltage applied to the inductor (kV), firing angle (α), Id is current flowing through the inductor (kA). Rc is equivalent commutating resistance (V) and Vd0 is maximum circuit bridge voltage (kV). Charge and discharge of SMES unit are controlled through change of commutation angle α [12].

In AGC operation, the dc voltage Ed across the superconducting inductor is continuously controlled depending on the sensed error signal of that area. Moreover, the inductor current deviation is used as a negative feedback signal in the SMES control loop. So, the current variable of SMES unit is intended to be settling to its steady state value. If the load is used as a negative feedback signal in the SMES control demand changes suddenly, the feedback provides the prompt restoration of current. The inductor current must be restored to its nominal value quickly after a system disturbance, so that it can respond to the next load disturbance immediately. As a result, the energy stored at any instant is given by

$$W_L = LI_d^2 / 2 \qquad MJ$$

(44)

Where L = inductance of SMES, in Henry)
Equations of inductor voltage deviation and current deviation for each area in Laplace domain are as follows:

$\Delta E_{di}(s) =$

$$\left((\frac{K_{SMES}}{1 + sT_{dci}})[\beta_1 \Delta F_1(s) + \Delta P_{tie1}(s)] - \frac{K_{id}}{1 + sT_{dci}} \Delta I_{di}(s) \right) \qquad (45)$$

$\Delta I_{di}(s) = (1/sLi)*\Delta Edi(s)$ (46)
Where,

$\Delta E_{di}(s)$ = converter voltage deviation applied to inductor in SMES unit

K_{SMES} = Gain of the control loop SMES

T_{dci} = converter time constant in SMES unit

K_{id} = gain for feedback ΔId in SMES unit.

$\Delta I_{di}(s)$ = inductor current deviation in SMES unit

The deviation in the inductor real power of SMES unit is expressed in time domain is as follow

$\Delta P_{SMESi} = \Delta E_{di}I_{doi} + \Delta I_{di}\Delta E_{di}$ (47)

In a two-area interconnected thermal power system even due to sudden small disturbances will continuously disturb the normal operation of power system. As a result the requirement of frequency controls of areas beyond the governor capabilities SMES is located in the area under disturbance absorbs and supply required power to compensate the load fluctuations.

7. CPSOISE CONTROLLER DESIGN

Craziness Particle Swarm Optimization (CPSO) is a population based on stochastic optimization technique developed by Kennedy and Eberhat in 1995 [20]. This method finds an optimal solution by simulating social behaviour of bird flocking. The population of the potential solution is called swarm and each individual solution within the swarm is called a particle. Particles in CPSO fly in the search domain guided by their individual experience and the experience of the swarm. Each particle knows its best value so far (pbest) and it's x, y position. This information is an analogy of the personal experience of each particle. More over each agent knows the best value so far into group (gbest) among pbests. This information is an analog of the knowledge of how the other particles around them have performed. Each particle tries to modify its position using this information : the current positions (x1, x2,… xd), the current velocities (V1, V2,…,Vd), the distance between the current position and pbest and the distance between the current position and gbest. The velocity is a component in the direction of previous motion (inertia). The movement of the particle towards the optimum solution is governed by updating its position and velocity attributes. The velocity and position update equation are given as [21].

$$v_i^{t+1} = v_i^t = c_1 r_1 (p_i^t - x_i^t) + c_2 r_2 (g_i^t - x_i^t) \qquad (48)$$

7.1. Craziness Particle Swarm Optimization

CPSO algorithm was also introduced by Kennedy and Eberhart to allow the CPSO algorithm to operate in problem spaces [21]. It uses the concept of velocity as a probability that a bit (position) takes on one or zero. In CPSO updating a velocity remains the same as the velocity in basic CPSO; however, the updating position is redefined by the following rule

$$S_i^{k+1} = \left\{ \begin{array}{ll} 0 & \text{if } r_3 \geq S(v_i^{k+1}) \\ 1 & \text{if } r_3 < S(v_i^{k+1}) \end{array} \right\} \qquad (49)$$

With r3~U (0,1) and S(0) is a sigmoid function for transforming the velocity to the probability constrained to the interval [0.0, 1.0] as follows

$$sig\,(v_i^k) = \frac{1}{1 + \exp\,(-v_i^k)} \qquad (50)$$

Where S (v) $\in$ (0,1) , S (0) = 0.5, and r3 is a quasi random number selected from a uniform distribution in [0.0, 1.0]. For a velocity of 0, the sigmoid function returns a probability of 0.5, implying that there is a 50% chance for the bit to flip.

The control area performance in any interconnected power system is analyzed with the interchange power flow, system frequency and other standards [22]. Apart from the standard deviation of Area Control Error (ACE) another way of measuring the control performance standard which is denoted as MAC is being adopted in this paper. When there is no correlation between the ACEs of the interconnected power system, the standards deviation of ACE which should be proportional to the square root of its capacity divided by the total capacity of the inter connected power system called as permitted values of the standard deviation of ACE of the Entire system was found to be less than the permitted value [22]. To over come this drawback, CPSOMAC criterion was adopted to evaluate the performance of the system.

MAC is defined by the following equation. ΔP_T is positive in the direction from its own system to the other system.

$$\mathbf{MAC=} \;\int\!\!(\alpha.\Delta f.\Delta P_T)dt \qquad (51)$$

In MAC, since the positive/negative of $\int \Delta f \times \Delta P_T$ is judged, (51) is equivalent to the following equation.

$$\mathbf{MAC} = \frac{\Sigma(\Delta f \; x \; \Delta P_T)}{\sqrt{\Sigma\Delta f^2 \; x \; \Sigma\Delta P_T^2}} \qquad (52)$$

From (31), the discrimination by MAC is equivalent to judging the area of $\Delta f \times \Delta P_T$.

Mathematically, MAC can be transformed into the following equation from (50) using ACE_A and ACE_B and it is assumed that P, P_A and P_B are constant [18]

$$\mathrm{MAC} \;\; = \;\; \frac{\overset{N}{\Sigma}ACE.(P_B ACE_A \; P_A ACE_B)}{N\sigma_{\Delta f}\sigma_{\Delta PT}KP.P} \qquad (53)$$

$$= \frac{\overset{N}{\Sigma}(P_B ACE_A^2 \; P_A ACE_B^2 + (P_B \; P_A) ACE_A ACE_B)}{N\,KP^2\sigma_{\Delta f}\,\sigma_{\Delta PT}}$$

$$= \frac{P_B\sigma_{ACE_A}^2 \; P_A\sigma_{ACE_B}^2}{\sigma_{\Delta f}\sigma_{\Delta P_T}KP^2} \;\; + $$

$$\frac{(P_B \; P_A)R_{ACE_{AB}}}{\sigma_{\Delta f}\sigma_{\Delta P_T}KP^2} \qquad (54)$$

If MAC is smaller than 0, then equation (54) will be expressed by the following equation
Hence

$$\mathrm{MAC} \;\; = \;\; -P_A\sigma_{ACE}^2 + P\sigma_{ACE_A}^2 + PR_{ACE_{AB}} \;\; \le \;\; 0 \qquad (55)$$

$$\sigma_{ACE_A}^2 \;\; \le \;\; \frac{P_A}{P}\sigma_{ACE}^2 - R_{ACE_{AB}} \qquad (56)$$

When there is no correlation between the ACEs, the evaluation by MAC becomes the same as the evaluation by the standard deviation of ACE. However, as there is no reference value to evaluate a generation control in MAC, the evaluation by MAC becomes a relative one between control areas.

Decentralized optimum proportional and integral controllers for the interconnected power systems are designed by suitably adopting the Integral Performance Index criterion. A characteristic of this criterion is that it weights large errors heavily and small errors lightly [7].

To obtain the optimum decentralized controller gain k_i (i=1, 2 …N), the following quadratic performance index is considered.

$$J_i = \int_0^t (\mathbf{x}_{ei}{}^T \mathbf{w}_i \mathbf{x}_{ei})\,dt \qquad i=1,2,\dots, N \qquad (57)$$

Where $\mathbf{x}_{ei}{}^T = [\,\Delta f_i\;]$

7.2 Decentralized Proportional Controllers Design

In the absence of the integral control one can sharply increase the gain of the closed loop system and thereby improve the system response. If the feedback gain of the integral controller is sufficiently high, overshoot will occur, increasing sharply as a function of the gain, which is highly undesirable. Thus, the integral controller gain cannot be higher because it leads to instability in the transient region [26]. Therefore the design of decentralized proportional controller considered first.

The optimum proportional controller feedback gain $k_{P\,CPSOISE}$ is obtained by plotting the cost curve for various values of k_P against the cost function of area i, J_i. The cost function of area i, J_i is obtained by simulating the closed loop system for various values of k_P and keeping k_I equal to zero throughout.

7.3 Decentralized Proportional Plus Integral Controller Design

Following the procedure discussed in the section 5.1, the integral controller is also designed. The cost function of area i J_i is obtained by simulating the closed loop system for various values of k_I and keeping k_P equal to $k_{P\,CPSOISE}$.

Following the procedure discussed in the section 5.1, the integral controller is also designed. The cost function of area i J_i is obtained by simulating the closed loop system for various values of k_I and keeping k_P equal to $k_{P\,CPSOISE}$.

8. CPSOASV CONTROLLER DESIGN

The closed stability of the system with the decentralized controllers are assessed using the settling time of the system output response. It is observed that the system whose output response settles fast will have minimum settling time and the apex stability verge. The minimum settling time or apex stability verge can be expressed as

$$f(K_P,K_I) = \min\,(\tau_{si}) \qquad (58)$$

where τ_{si} is the settling time of the output response of (Δf_i) frequency deviation of the " i^{th} " area

8.1 Decentralized Proportional Controller Design

The Proportional Controller feed back gain $K_{P(ASV)}$ is obtained on the basis of the Apex Stability Verge criterion by plotting the maximum stability curve for various values of K_P against the settling time of Δf_i . The integeral feed back gain K_I is treated as zero throughout this design.

8.2 Decentralized Proportional Plus Integral Controller Design

The Proportional plus Integral Controller feed back gains are obtained by plotting the settling time curve for various values of K_I keeping $K_P = K_{P(ASV)}$

9. DECENTRALIZED CONTROLLER USING MULTI-OBJECTIVE CRAZINESS PARTICLE SWARM OPTIMIZATION DESIGN

The success of the Particle Swarm Optimization (CPSO) algorithm as a single objective optimizer [20, 21] has motivated to extend the use of optimization algorithm Multi-Objective problems for the load frequency control problems. In problems with more than one conflicting objective, there exist no single optimum solution rather there exists a set of solutions which are all optimal involving trade-offs between conflicting objective (pareto optimal set)[23-25].

If an element in archive is dominated by a new solution, the corresponding element in archive is removed. If new solution is not dominated by any element in archive, new solution is added to archive. If archive is full, crowding, distance between elements in archive are computed according to [21] and then one element in archive is selected to remove according to diversity.

In (48) each particle need to gbest for motioning in search space. In Multi-Objective CPSO a set of gbests that called archive there exists many different ways to select gbest. In our method, gbest is selected from archives based on crowding distance to maintain diversity. If an element in archive has more diversity, it has more chance to be selected as gbest. Roulette wheel selection is used to do it. So the particles motion to pareto optimal set and diversity is maintained with roulette wheel selection for selecting gbest.

9.1 Particle Swarm Optimization Algorithm

Step 1: Initialise searching point and velocity are randomly generated within their limit.

Step 2: pbest is set to each initial searching point. The best-evaluated values among Pbest is set to g_{best}.

Step 3: New velocity are calculated using the equation.

$V_i^{k+1} = w_i v_i^k + C_1 * rand()*(pbest_{id} - S_i^k) + C_2 * rand()*(gbest_d - S_i^k)$

Step 4: if $V_{id}^{(t+1)} < V_{dmin}$ the $V_{id}^{(t+1)} = V_{dmin}$ and if $V_{id}^{(t+1)} > V_{dmax}$ then $V_{id}^{(t+1)} = V_{dmax}$

Step 5: New searching point are calculated using the equation, $S_i^{k+1} = Si^k + V_i^{k+1}$

Step 6: Evaluate the fitness values for new searching point . if evaluated values of each agent is better than previous pbest then set to pbest, if the best pbest is better than gbest then set to gbest.

Step 7: If the optimal solution is reached stop the process, otherwise goto step 3.

10. SIMULATION RESULTS AND OBSERVATIONS

With the consideration of Mutual Aid criterions (MAC) the CPSO based load frequency controller for the two area power system with SMES units considering GDB and GRC nonlinearities interconnected through TCPS are designed and implemented. Simulation is carried out to design the Proportional plus Integral controller for 0.01 p.u MW step load change in area 1 and corresponding responses for change in frequencies, change in tie-line power flow and change in input power are obtained. From simulation results as shown in figure 4 it is found that the controller designed using

MOCPSO for areas interconnected with TCPS exhibit better transient and steady state performance when compared with the output response obtained with the controllers designed using CPSOISE for areas interconnected with TCPS.

Table 1. Controller Design using CPSOISE, CPSOASV and MOCPSO criterion.

Controller Design using **CPSOISE** criterion		
K_P=2.01		K_I=1.24
J=0.0621		
Settling Time (Sec)		
ΔF_1=35.98	ΔF_2=32.09	$\Delta P_{tie\ TCPS}$=34.77

Controller Design using **CPSOASV** criterion		
K_P=1.26		K_I=0.96
J=0.0734		
Settling Time (Sec)		
ΔF_1=15.20	ΔF_2=16.05	$\Delta P_{tie\ TCPS}$=15.07

Controller Design using **MOCPSO** criterion		
K_P=1.42		K_I=1.03
J=0.0603		
Settling Time (Sec)		
ΔF_1=18.17	ΔF_2=16.73	$\Delta P_{tie\ TCPS}$=16.94
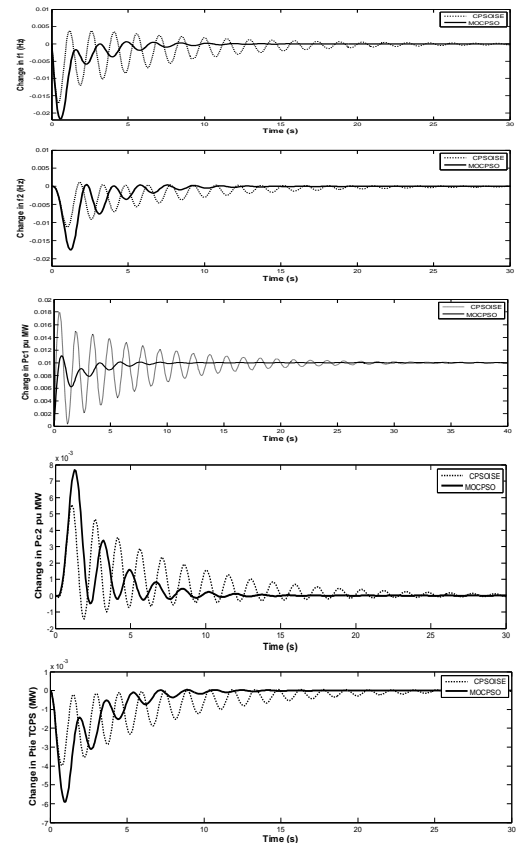
Fig 4. Frequency Deviations, Control Input Deviations and Tie-Line Power Deviation of a Two area Power System with SMES Interconnected coordinated with TCPS in the tie-line for 1% Step Load Change in Area 1.

11. CONCLUSIONS

Analysis of load frequency control models of interconnected power system   representation with SMES Units considering GDB and GRC nonlinearities interconnected through TCPS provide more detailed information about the system evolution of the frequency of each individual control area and the power interchanged through each tie-line has been prsented.

The proportional plus Integral Controllers namely CPSOISE, ASV controllers for the two area power system with SMES units considering GDB and GRC nonlinearities interconnected through TCPS with are designed and the above two controller's gains are used as the upper & lower or lower and upper limits for the proposed MOCPSO controller. The multi-objective CPSO criterion based controllers is designed for 1% step load disturbance in area 1.

From the simulated results it is found that the MOCPSO based controllers designed for power systems with SMES units considering GDB and GRC nonlinearities interconnected through TCPS show better improved system performance than that of the controller designed using CPSOISE criterion.

12. ACKNOWLEDGEMENT

13. REFERENCES

[1] B . Shayeghi, H. A. Shayanfar, A. Jalili, "Load frequency Control Strategies: A state-of-the-art survey for the researcher", *Energy Conservation and Management*, Vol. 50(2), pp. 344-353, 2009.

[2] I. Ibraheem, P. Kumar,   DP. Kothari, "Recent Philosophies of Automatic Generation Control Strategies in Power Systems" *IEEE Transactions on Power Systems*, pp. 346-357, 2005.

[3] L. Basanez, J. Riera, J. Ayza, "Modeling and simulation of Multi area Power System Load frequency Control" *Mathematics and computers in Simulation*, PP. 54-62, 1984.

[4] Janardan Nanda, Ashish Mangla, Sanjay Suri, "Some new findings on Automatic Generation Control of an interconnected hydrothermal system with conventional controllers", *IEEE Transactions on Energy Conversion*, Vol. 21(1), pp.187-194, 2006 .

[5] I. A. Chidambaram, S. Velusami, "Design of Decentralized Biased Controllers for Load-Frequency Control of Interconnected Power Systems", *Electric Power Components and Systems*, Vol. 33, PP. 1313-1331, 2005.

[6] I. A. Chidambaram, S.Velusami, "Design of decentralized biased dual mode controllers for load-frequency control of interconnected power systems considering GDB and GRC nonlinearities", *International Journal of Energy Conversion and Management (Elsevier)*, Vol. 48, pp.1691-1702, 2007.

[7] Gayadhar Panda, Sidhartha Panda, Cemal Ardil, "Automatic Generation Control of Interconnected Power System with Generation Rate Constraints by Hybrid Neuro Fuzzy Approach", *World Academy of Science, Engineering and Technology*, Vol. 52, pp.543-548, 2009.

[8] I. A. Chidambaram, S. Velusami, "Design of decentralized biased controllers for load-frequency control of interconnected power systems considering governor deadband nonlinearity", *IEEE International Conference (INDICON 2005)*, Chennai, pp. 521-525, December 2005.

[9] B. Paramasivam, R. Arivoli, I. A. Chidambaram, "Design of GA based decentralized controller for Load-Frequency Control of interconnected power systems considering Thyristor controlled phase shifter (TCPS) in the tie-line", *UGC sponsored National Conference on Planning, Operation and Control of interconnected Power Systems*, Annamalai University, Annamalainagar, pp. 66-76, March 2009.

[10] S. C. Tripathy, Balasubramanian, and P. S. Chandramohanan Nair "Effect of superconducting magnetic energy storage in power systems", *IEEE Transactions on Power systems*, Vol. 7. No. 3, pp. 1266-1273, Aug. 1992.

[11] R. J. Abraham, D. Das and A. Patra, "Automatic Generation Control of an Interconnected Hydrothermal Power System Considering Superconducting Magnetic Energy Storage", *Electrical Power and Energy Systems*; 29, pp. 271-579, 2007.

[12] Sathans Suhag and Akhilesh Swarup, "Automatic Generation Control of Multi-Area Multi Unit Power System with SMES using Fuzzy Gain Scheduling Approach", *International Journal of Research and Reviews in Electrical and Computer Engineering (IJRRECE)*, Vol. 1, No. 2, pp. 83-91, June 2011.

[13] Pal, B. C., Coonick, A. H., and Macdonald, D. C.: 'Robust damping controller design in power systems with superconducting magnetic energy storage devices', IEEE Trans. Power Syst., 15, (1), pp. 320–325, 2000.

[14] Rajesh Joseph Abraham; Das, D.; and Patra, A., "AGC Study of a Hydrothermal System with SMES and TCPS", *European Transactions on Electrical Power,* 2008; DOI: 10. 1002/etep. 235, 2008.

[15] Mairaj Uddin Mufti, Shameem Ahmad Lone, Sheikh Javed Iqbal, Imran Mushtaq, "Improved Load Frequency Control with Superconducting Magnetic Energy Storage in Interconnected Power System", *IEEJ Transaction*, Vol. 2, pp. 387-397, 2007.

[16] Baker, R., Guth, G., Egli, W., and Eglin, P.: 'Control algorithm for a static phase shifting transformer to enhance transient and dynamic stability of large power systems', *IEEE Trans. Power Appar. Syst.*, 1982, 101, (9), pp. 3532–3542.

[17] Wang HF.; Shift FJ.; Li M., "Analysis of Thyristor Controlled Phase Shifter Applied in Damping Power System Oscillations", *International Journal of Electrical Power and Energy Systems,* 19:1–9, 1997.

[18] R. J. Abraham, D. Das, A. Patra, "AGC of a hydrothermal system with thyristor controlled phase shifter in the tie-line", *IEEE Transaction on Power Systems*, 2006: 0-7803-9525, 2006.

[19] Y. L. Karnavas, and D. P. Papadopoulos, 'AGC for autonomous power system using combined intelligent techniques', *Int. J. Electr. Power Syst. Res.*, 2002, 62, pp. 225–239, 2002.

[20] J. Kennedy and R. Eberhart, "Particle swarm optimization", Neural Networks, 1995. Proceedings., *IEEE International Conference on* Neural networks vol. 1, pp 1942-1948, vol. 4, 1995.

[21] M. Clere, J.Kennady, "The particle swarm explosion, stability and convergence in multi dimensional complex space," *IEEE Transaction Evolutionary Computation*, vol. 6, pp. 58-73, 2002.

[22] Tetsuo Sasaki, KazuhiroEnomoto, "Statistical and Dynamic Analysis of Generation control performance standards," *IEEE Transactions on Power Systems*, Vol. xx PP 100-105, 2001.

[23] Davoud Sedighizadeh and Ellips Masehian, "Particle Swarm Optimization Methods, Taxonomy and Applications," *International Journal of Computer Theory and Engineering*, Vol. 1, No. 5, pp.1793-8201, 2009.

[24] Margarita Reyes-Sierra and Carlos A. Coello-Coello, "Multi-Objective Particle Swarm Optimizers: A Survey of the State-of-the-Art", *International Journal of Computational Intelligence Research*, Vol. 2, No. 3, pp. 287–308, 2006.

[25] SL.Ho, S. Yang, G. Ni,E.Wc.Lo, H.C. Wong."A Particle Swarm Optimization based method for multi-objective design optimization based method for multi- objective design optimization," *IEEE Transaction on magnetic*, vol. 41 (5), pp. 1756-1759, 2005.

[26] Katsuhiko Ogata, Modern Control Engineering, Prentice Hall of India Private Limited, New Delhi, India, July 1986.

APPENDIX – A

(i)   Data for Thermal Power System with Reheat Turbines considering GDB and GRC nonlinearities [6].
Rating of each area = 2000 MW, Base power = 2000 MVA, f^o = 60 Hz, $R_1 = R_2 = 6.0$ Hz / pu MW, $T_{g1} = T_{g2} = 0.1$ sec, $T_{r1} = T_{r2} = 10$ sec, $T_{t1} = T_{t2} = 0.3$ sec, $K_{p1} = K_{p2} = 120$ Hz / pu MW, $K_{r1} = K_{r2} = 0.5$, $T_{p1} = T_{p2} = 20$ sec, $_1 = _2 = 0.1675$ pu MW / Hz, $T_{12} = 0.50$ pu MW / Hz, $a_{12} = -1$, $P_{D1} = 0.01$ pu MW, $N_1 = 0.8$, $N_2 = -0.2$,

$\Delta P_{gmax} = 0.1$ pu MW / min, T=2sec (normal sampling rate)

(ii)   Data for SMES[10]
$I_{d0} = 5$kA.
$k_0 = 50$kV/unit ACE.
kid = 0.20kV/kA.
L = 2H.

(iii)   Data for TCPS[18]
$T_{PS} = $ 0.1s
$K_\phi = $ 1.5 rad/Hz
$\phi_{max} = 10^0$
$\phi_{min} = -10^0$

NOMENCLATURE

a_{12}	$-Pr_1 / Pr_2$
ACE	Area control error of area
AGC	Automatic Generation Control
β_i	Frequency bias constant
β_i	$(D_i + 1/R_i)$ area frequency response characteristics
CPSOASV	Craziness Particle Swarm Optimization based Apex Stability Verge
f	Rated Frequency
H_i	Inertia Constant
K_I	Integral gain
K_p	Proportional gain
LFC	Load Frequency Control
MAC	Mutual Aid Criterion
MOCPSO	Multi Objective Craziness Particle Swarm Optimization.
CPSOISE	Craziness Particle Swarm Optimization based Integral Square Error Criterion.
ΔP_{Di}	Incremental load consumption in area i
ΔP_{tiei}	Power deviation of the interchange between area i
T_{12}	Synchronizing power coefficient

AUTHOR BIOGRAPHICS

R. Arivoli (1959) received Bachelor of Electrical and Electronics Engineering (1991) Master of Engineering in Power System Engineering (1999) from Annamalai University, Annamalainagar. During 1992 - 2007 he was working as Lecturer in the Department of Electrical Engineering, Annamalai University and now he is working as Associate Professor, Department of Electrical Engineering, Annamalai University- Annamalainagar. He is currently pursuing Ph.D degree in Electrical Engineering at Annamalai University. Annamalainagar. His research interests are in Power Systems, Electrical Measurements. Electrical Measurements Laboratory, Department of Electrical Engineering,   Annamalai University, Annamalainagar – 608002, Tamilnadu, India,

I. A. Chidambaram (1966) received Bachelor of Engineering in Electrical and Electronics Engineering (1992) and Ph.D in Electrical Engineering (2007) from Annamalai University, Annamalainagar. During 1988 - 1993 he was working as Lecturer in the Department of Electrical Engineering, Annamalai University and from 2007 he is working as Professor in the Department of Electrical Engineering, Annamalai University, Annamalainagar. He is a member of ISTE. His research interests are in power systems, electrical measurements and control systems. Electrical Measurements Laboratory, Department of Electrical Engineering, Annamalai University, Annamalainagar 608002, Tamilnadu, India,